INTERNATIONAL JOURNAL OF CLIMATOLOGY
Int. J. Climatol. (2016)
Published online in Wiley Online Library
(wileyonlinelibrary.com) DOI: 10.1002/joc.4813

RMetS
Royal Meteorological Society

Short Communication

A new method to classify ENSO events into eastern and central Pacific types

Hye-In Jeong[a,b] and Joong-Bae Ahn[b]*
[a] *Climate Research Department, APEC Climate Center (APCC), Busan, Republic of Korea*
[b] *Division of Earth Environmental System, Pusan National University, Busan, Republic of Korea*

ABSTRACT: In order to clearly classify El Niño–Southern Oscillation (ENSO) events into eastern Pacific (EP) and central Pacific (CP) types, we develop two new indices defined as pattern correlation coefficients (PCCs) between monthly sea surface temperature (SST) anomalies (SSTAs) and first two leading empirical orthogonal function modes of tropical Pacific (20°S–20°N, 110°E–70°W) SSTAs. These new indices not only show close relationships with ENSO indices derived from several previous methods, but also demonstrate reasonable abilities to distinguish between two types of ENSO event. The major characteristic features of the EP-type and CP-type ENSO forcings are well captured from SST responses regressed onto each new index. Furthermore, the monthly frequencies of occurrences derived from two indices are quite similar to variation patterns of phase-locking behaviours of two types of ENSO event.

KEY WORDS eastern Pacific; central Pacific; two types of ENSO; SST response; phase lock; mature phase

Received 16 November 2015; Revised 12 May 2016; Accepted 30 May 2016

1. Introduction

Recently, a lot of attention has focused on two types of El Niño–Southern Oscillation (ENSO): the eastern Pacific (EP) type (alternately known as canonical), in which the maximum sea surface temperature (SST) variability appears over the equatorial EP, and the central Pacific (CP) type (alternately known as Dateline, Modoki, and Warm Pool), in which the significant SST anomalies (SSTAs) are mainly located in the CP near the date line (Larkin and Harrison, 2005; Ashok *et al.*, 2007; Yu and Kao, 2007; Kao and Yu, 2009; Kug *et al.*, 2009, 2010).

Several studies have indicated that impacts by the EP-type and CP-type ENSO forcing may differ distinctly in various climate elements such as regional monsoon rainfall (Kumar *et al.,* 2006; Ashok *et al.,* 2007; Wang and Hendon, 2007; Taschetto and England, 2009; Mo, 2010; Feng and Li, 2011; Weng *et al.,* 2011; Zhang *et al.,* 2011), temperature (Ashok *et al.,* 2007; Mo, 2010; Weng *et al.,* 2011), storm track activity (Ashok *et al.,* 2009), and tropical cyclone activity (Kim *et al.,* 2009; Chen, 2011) in the Atlantic and western Pacific, and also play a significant role in the global climate variability. These studies illustrate that the proper classification of the two types of ENSO event is important in the understanding and interpretation of climate and its variability.

* Correspondence to: J.-B. Ahn, Division of Earth Environmental System, Pusan National University, 2, Busandaehak-ro 63beon-gil, Geumjeong-gu, Busan, 46241, Republic of Korea. E-mail: jbahn@pusan.ac.kr

However, as suggested by Trenberth and Stepaniak (2001) and Kao and Yu (2009), the indices have a problem currently in classifying the ENSO events into EP and CP types, which necessitates the development of new ENSO indices that can describe better and distinguish between these two types of ENSO event. Accordingly, a new classification method to distinctly separate the ENSO-related variability into two types is suggested. To check the suitability of ENSO indices classified by the new method, we investigate not only the unique response related to the corresponding SST forcing but also intrinsic properties such as the phase locking and the frequency of occurrence for two types of ENSO event.

2. Data and methodology

2.1. Data

The extended reconstructed SST (ERSST.v3b) data sets (Smith *et al.*, 2008) from January 1982 to December 2014 are used in this study. For verification, we also utilize optimally interpolated SST (OISST) data sets (Reynolds *et al.*, 2002) for the same period. The OISST monthly data are interpolated to $2° \times 2°$, which has the same resolution of ERSST data set.

2.2. Existing classification methods for ENSO event

To better understand the different type of ENSOs, Capotondi *et al.* (2015) have introduced several ENSO indices by constructing various climate variables

such as SST (Ashok *et al.*, 2007; Kao and Yu, 2009; Kug *et al.*, 2009; Ren and Jin, 2011; Takahashi *et al.*, 2011), subsurface ocean temperature (Yu *et al.*, 2011), sea surface salinity (Singh *et al.*, 2011), or outgoing longwave radiation (Chiodi and Harrison, 2013). Among them, several ENSO indices utilizing SSTA are selected to compare with our new index introduced in Section 2.3.

Ashok *et al.* (2007) used the Niño3 and ENSO Modoki index (EMI) to distinguish between EP-type and CP-type ENSO events, respectively. The latter was derived based on the second empirical orthogonal function pattern (EOF2) of the SSTA over the tropical Pacific. More specifically, they defined the CP-type ENSO as the case which the amplitude of the index is equal to or greater than 0.7σ, where σ is its standard deviation. The EP-type ENSO event refers the case which the amplitude of the index is equal to or greater than 1σ. This classification method is referred to as 'AS' method in this study.

Kao and Yu (2009) suggested EP and CP indices using a combined regression-EOF procedure to separate two types of ENSO. To obtain the EP index, they first subtracted the anomalies regressed on the Niño4 index from the original SSTA before applying the EOF analysis. Similarly, they subtracted the SSTA regressed on the Niño1 + 2 index from the original SSTA before the EOF analysis to identify the leading structure of the CP ENSO. Each normalized leading principal component (PC1) was defined as EP or CP index. The ENSO state was regarded as the EP (CP) type when the value of each index is equal or larger than 1. This classification method is referred to as 'KY' in our study.

In the method of Kug *et al.* (2009), Niño3 and Niño4 indices were used to classify El Niño events into EP and CP El Niño groups, respectively. The EP (CP) El Niño events defined as years in which the Niño3 (Niño4) SST index is larger than the Niño4 (Niño3) SST index and it is greater than its standard deviation. Henceforth, we refer this method as the 'KU' method.

More recently, Ren and Jin (2011) proposed new Niño indices (Nct and Nwp) to distinguish between two types of ENSO event. These two new indices are defined as a linear combination of Niño3 and Niño4 indices, which are conditioned by the ENSO phase. This method (henceforth the 'RJ' method) defines the EP (CP)-type ENSO event when the Nct (Nwp) index is greater than 1σ. Using this method, they found an increasing prevalence of CP-type ENSO since 1990 and a regime shift in ENSO at 1976/1977.

At around the same time as Ren and Jin (2011), Takahashi *et al.* (2011) also defined new E and C ENSO indices. They used two orthogonal axes, which are rotated 45° relative to the EOF of SSTA in the tropical Pacific using the sum and the difference of the first two PC timeseries. ENSO events are separated into two groups by this method. One represents the EP El Niño and the other represents both central Pacific El Niño and La Niña events. We refer to this methodology as 'TA' in our study.

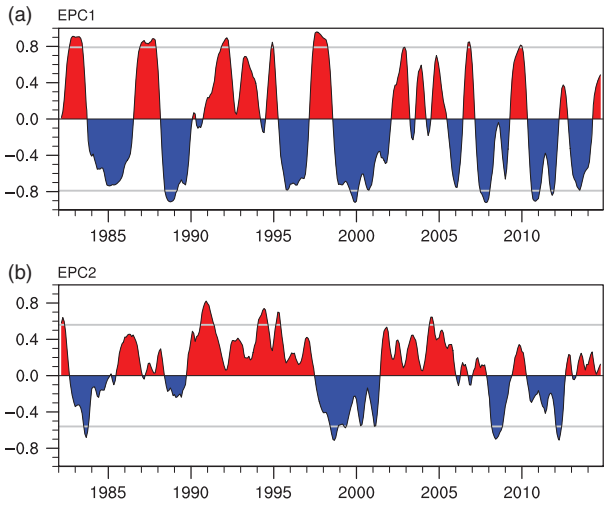

Figure 1. Time series of the 5-month running mean of PCCs between first two leading EOF modes of SSTAs and SSTAs over the tropical Pacific (20°S–20°N, 110°E–70°W) for the period January 1982 through December 2014. Horizontal reference lines (grey) represent significant PCCs at the 90% confidence level.

2.3. New classification of ENSO event

A new classification method to distinguish between EP-type and CP-type ENSO events is proposed in this study. The canonical EP-type ENSO has a well-known pattern of the SSTA retaining the same sign throughout the equatorial EP with a maximum at around 155°–115°W. The CP-type ENSO presents the peculiar warming in the central equatorial Pacific flanked by colder SSTAs on both sides along the equator. These EP-type and CP-type ENSO patterns are represented in the first and second EOF modes of tropical Pacific SSTA, respectively (Ashok *et al.*, 2007; Jeong *et al.*, 2012, 2015). Based on fundamental features associated with this concept, we first carry out the EOF analysis using the monthly SSTA over the tropical Pacific (20°S–20°N, 110°E–70°W) from 1982 to 2014, and obtain the first and second EOF modes of monthly SSTAs as EP-type and CP-type ENSO modes (figures not shown), respectively. The pattern correlation coefficients (PCCs) between first two leading EOF modes and monthly mean SSTA are then calculated for the period January 1982 through December 2014. To smooth out short-term fluctuations such as intraseasonal variations, the 5-month running mean is applied to the above-mentioned PCCs. Finally, we obtain the EOF-based pattern correlations for two EOF modes, which are referred to as EPC1 and EPC2 for the first and second modes, respectively (Figure 1). The EP (CP)-type El Niño is defined as the case when the EPC1 (EPC2) index is equal to or greater than 0.79 (0.57), which is significant at the 90% confidence level from the two-tailed Student's *t*-test. According to this method, the EP (CP)-type La Niña state is defined as the case when the EPC1 (EPC2) index is equal to or less than −0.79 (−0.57). This new classification method is referred to as 'JA' method in our study. As shown in Figure 1(a), the strongest El Niño events (such as those occurred in 1982–1983 and 1997–1998) are classified as the EP-type

Table 1. Inter-temporal correlations between EP-type ENSO indices obtained from one method and those from other methods (upper triangle). Inter-temporal correlations between CP-type ENSO indices obtained from one method and those from other methods (lower triangle). All correlation coefficients are significant at the 95% confidence level.

	JA	AS	KY	KU	RJ	TA
JA		0.89	0.38	0.89	0.82	0.81
AS	0.90		0.58	1.00	0.98	0.93
KY	0.77	0.90		0.58	0.71	0.79
KU	0.63	0.71	0.76		0.83	0.93
RJ	0.81	0.88	0.81	0.98		0.95
TA	0.46	0.61	0.74	0.94	0.66	

El Niño reasonably well by the JA method. During last three decades, eight El Niño and nine La Niña episodes occurred as the EP type and five El Niño and five La Niña episodes occurred as the CP type.

3. Results

In this section, we compare the characteristics of the two types of ENSO classified by six classification methods mentioned above.

3.1. Classification of ENSO event into two types

Before discussing the classification of ENSO, we first investigate the temporal (monthly) correlations between our new indices from the JA method and indices obtained from various existing methods. As shown in Table 1, the EPC1 index of the JA method, which is representing the EP-type ENSO, is significantly correlated with indices from the other five methods. As discussed in previous studies (Ashok *et al.*, 2007; Ren and Jin, 2011), the other five EP-type ENSO indices are also well correlated with each other.

The EPC2 index (CP-type ENSO) is highly correlated with EMI (0.90) from the AS method as EMI is basically defined by the EOF analysis over the equatorial Pacific basin. However, it shows the relatively low temporal correlation (0.46) with the C index from the TA method, even though the value is still significant.

In order to confirm how well and distinctly EP-type and CP-type ENSO events are separated, scatter diagrams of two types of ENSO indices for six different classification methods are shown in Figure 2. The x and y axes in each diagram of Figure 2 refer to EP-type and CP-type ENSO events, respectively. Each coloured area denotes EP-type El Niño (red), EP-type La Niña (blue), CP-type El Niño (yellow), and CP-type La Niña (green) events. Grey areas located at the corners of each diagram indicate the overlapped cases, not clearly classified by the methods, for two types of events. Unlike the other five methods, the TA method is designed to disentangle the EP-type El Niño event from CP-type El Niño and La Niña events (Figure 2(f)). We also represent temporal correlation coefficients (TCCs) between two ENSO indices at the top-right corner of each diagram as an indicator representing the separation between two indices of each method. Thus, the lower the TCC is, the better the separation between two indices is.

In all diagrams except TA method, monthly values are distributed in white boxes representing the neutral (normal) condition located between two types of La Niña and El Niño conditions. Generally, TCCs between two types of ENSO indices derived from three classification methods such as JA, AS, and RJ (0.23, 0.11, and 0.02, respectively) are considerably lower than those from KY, KU, and TA methods (−0.50, 0.70, and 0.65, respectively). Thus, two types of ENSO event are particularly well distinguished by three methods of JA, AS, and RJ.

In the case of the JA method, there are no overlapping cases between EP-type and CP-type ENSO events, indicating that indices derived from the JA method clearly classify individual ENSO events into EP type and CP type. Although AS and KY methods are based on the EOF analysis of SSTA over the tropical Pacific, there are numerous overlapping events between the types. In the RJ method which shows a relatively low TCC, many cases remain in the domains which are not clearly classified by the method, despite fewer events in overlapping zones compared with AS and KU methods.

3.2. Evaluation of six different ENSO indices using SST responses

As aforementioned in the introduction, ENSO phenomena, caused by the atmosphere−ocean interaction in the tropical Pacific, considerably affect the weather and climate variability in tropical and mid-latitude regions. Accordingly, it is very important to investigate how well SST responses to six different ENSO indices describe main features in the tropical and extratropical Pacific region. In this context, we compare regressed SSTA patterns on two types of ENSO index obtained from six different methods and observed composite fields of SSTA for EP-type and CP-type ENSO events. First of all, before carrying out the composite analysis for two types of ENSO event, we select seasonal EP-type and CP-type ENSO events which are classified in common by above six methods. However, for the case of CP-type ENSO events for the boreal winter (December through February; DJF) season, there are no commonly selected cases from six different methods because of the relatively rigorous criteria of the JA and TA methods. Instead, we performed the composite analysis

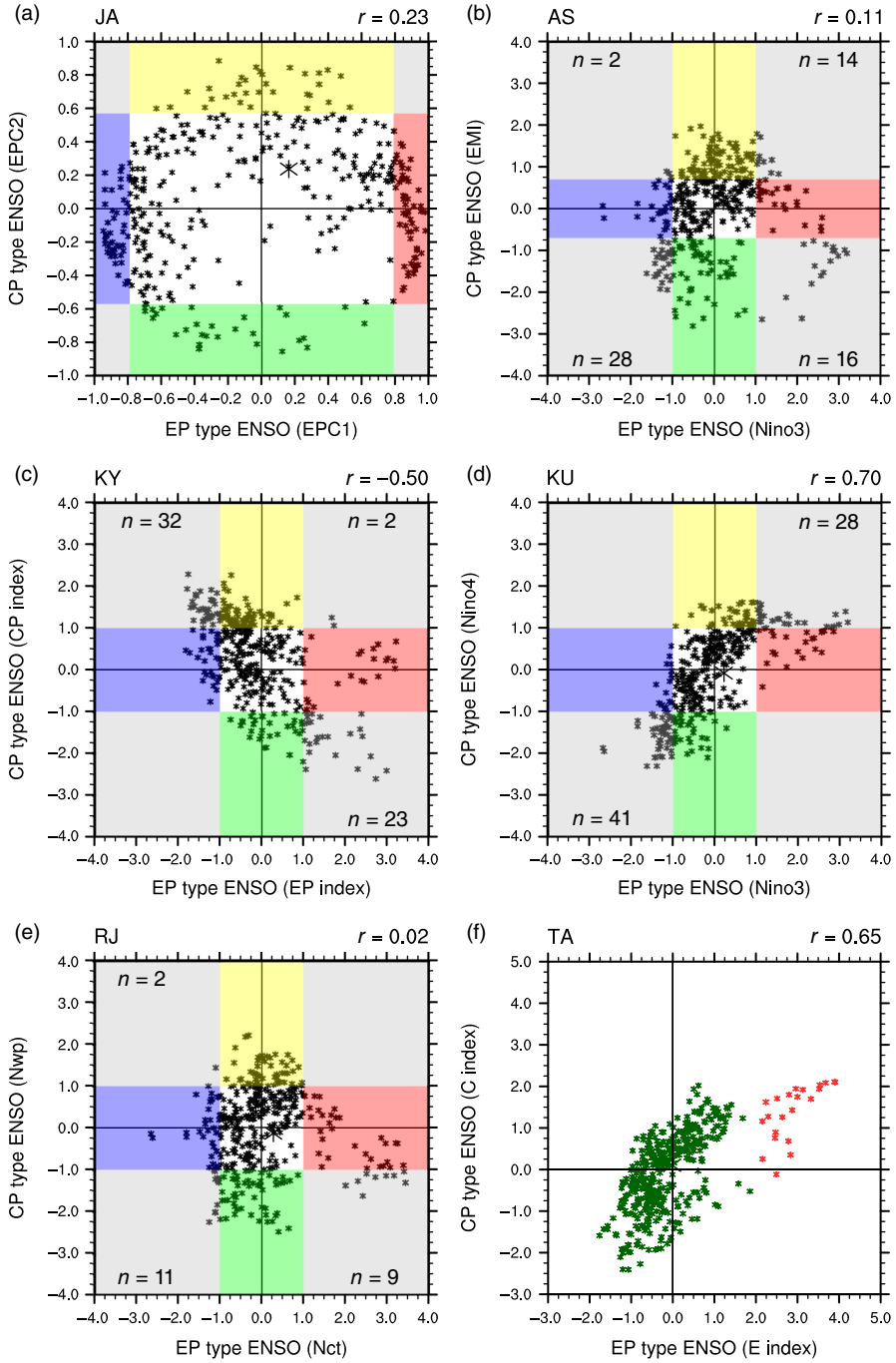

Figure 2. Scatter diagrams of two types of ENSO indices for six different classification methods (JA, AS, KY, KU, RJ, and TA method) during the period January 1982 through December 2014. To classify ENSO events into two types: (a) JA as a new classification method uses EPC1 and EPC2 indices, whereas (b) AS, (c) KY, (d) KU, (e) RJ, and (f) TA as existing classification methods employ the normalized Niño3 and EMI, EP, and CP indices, Niño3 and Niño4, Nct and Nwp, and E and C indices, respectively. The '*n*' in the grey boxes indicates the number of overlapping cases of two types of ENSO events. The '*r*' in the upper right corner of each panel denotes the correlation between two indices.

from the other four methods for CP-type ENSO events for the DJF season.

In comparison with the observed composite SSTA field, characteristic features of EP (CP) ENSO patterns are clearly portrayed in regressed SSTAs derived from six classification methods for each season (figure not shown).

For better understanding of the relationship between observed composite SSTA fields and six different regressed SSTA patterns for each season and ENSO type, spatial PCCs (Jolliffe and Stephenson, 2003) are calculated (Figure 3). We present spatial pattern correlations for each season and ENSO type over the following three specific regions: North Pacific (0°–60°N, 120°E–90°W), tropical Pacific (20°S–20°N, 110°E–70°W), and South Pacific (60°S–0°, 120°E–60°W). It is shown that regression patterns obtained from each EP-type ENSO signal, which is much more significant and stronger than the CP-type signal over the tropics, are similar to one another

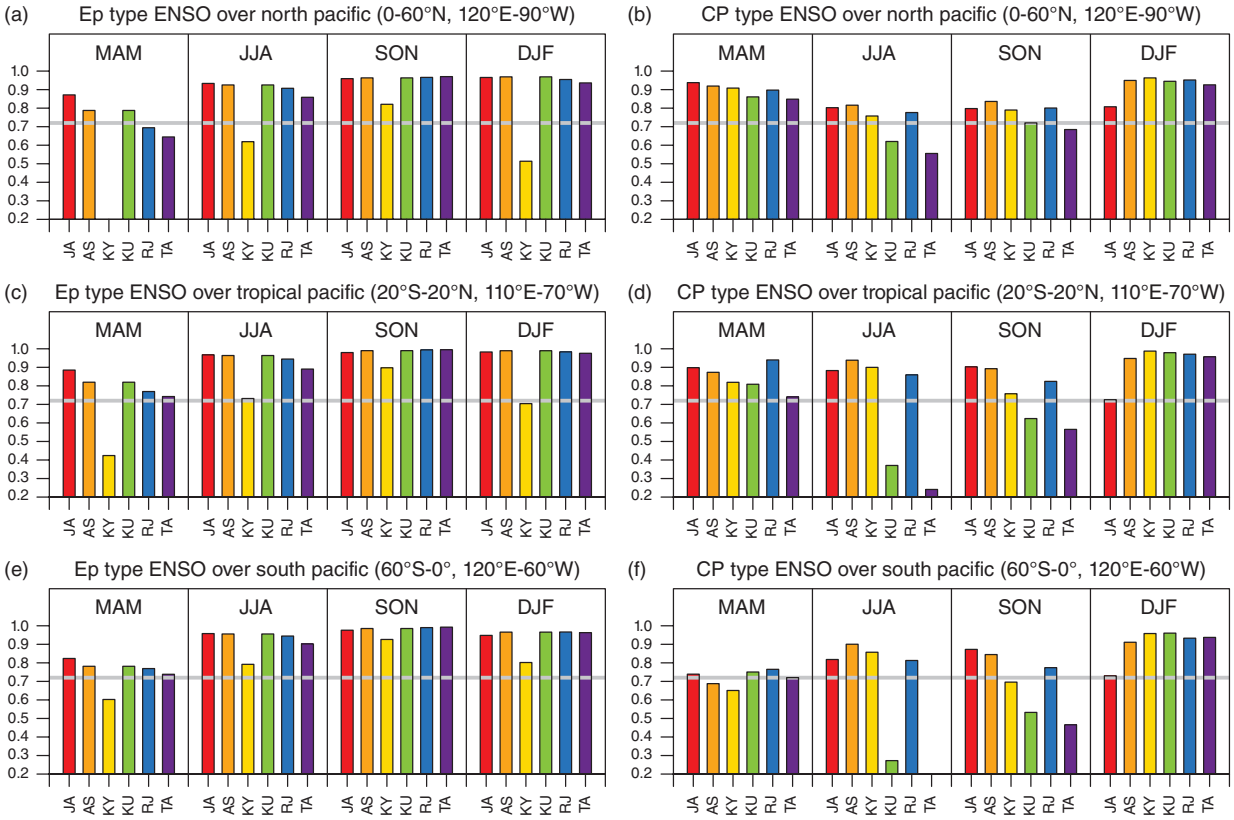

Figure 3. Spatial PCCs between SSTA patterns regressed on EP (left)-type and CP (right)-type ENSO indices from six different classification methods and the observed SSTA composites, using seasonal common cases selected from six methods, for two types of ENSO events over the (a, b) North Pacific (0°–60°N, 120°E–90°W), (c, d) tropical Pacific (20°S–20°N, 110°E–70°W), and (e, f) South Pacific (60°S–0°, 120°E–60°W) in each season. The grey line represents the significant value at the 90% confidence level from a two-tailed Student's *t*-test.

with little difference from the composite observation fields for all seasons except spring (March through May; MAM). In EP-type ENSO cases, spatial relationships for spring have a relatively lower for all regions compared with those for the other seasons, even though they are statistically significant at the 90% confidence level based on Student's two-tailed *t*-test. However, the spring SSTA pattern regressed onto EP-type ENSO indices obtained from the JA classification method shows a significantly higher correlation with the composite field of the observed SSTA during the MAM season than those from other methods (Figure 3(a)).

The PCCs of the SSTA response to the CP-type ENSO signal shows generally lower performances than those to the EP-type ENSO signal in three of four seasons. However, there exists a relatively higher spatial relationship than the response to the EP-type ENSO over the North Pacific region in spring.

The KU and TA methods show relatively lower PCCs in the CP-type ENSO among six different classification methods during boreal summer (June through August; JJA) and fall (September through November; SON) because EP-type and CP-type ENSO events are not clearly distinguished with these methods. This implies that the CP-type ENSO index from KU and TA methods describes inadequately special features over the central tropical Pacific. The high PCCs of more than 0.7 for all seasons between EP-type and CP-type ENSO events for observed composite fields and six regressed patterns of SSTAs in each season also prove the limitation of the method (Table 2).

Table 2. Pattern correlations between EP-type and CP-type ENSO events for observed composite fields and six regressed patterns of SSTAs in each season.

	MAM	JJA	SON	DJF
Composite field	0.64*	0.18	0.31	
JA	0.40	0.27	0.47	0.48*
AS	0.13	−0.20	0.68*	0.74**
KY	−0.61*	−0.55*	0.47	0.37
KU	0.81**	0.84**	0.96**	0.95**
RJ	0.26	0.06	0.68*	0.70*
TA	0.77**	0.81**	0.95**	0.94**

*,**Significant correlation coefficients at the 90 and 95% confidence levels, respectively.

Thus, the JA method can be regarded as the most reliable among ENSO classification methods and shows significant results at the 90% confidence level regardless of season, region, and ENSO type.

3.3. Statistical characteristics of two types of ENSO event classified by JA method

It is well known that the EP-type ENSO, which tends to reach its mature phase during the boreal winter, is

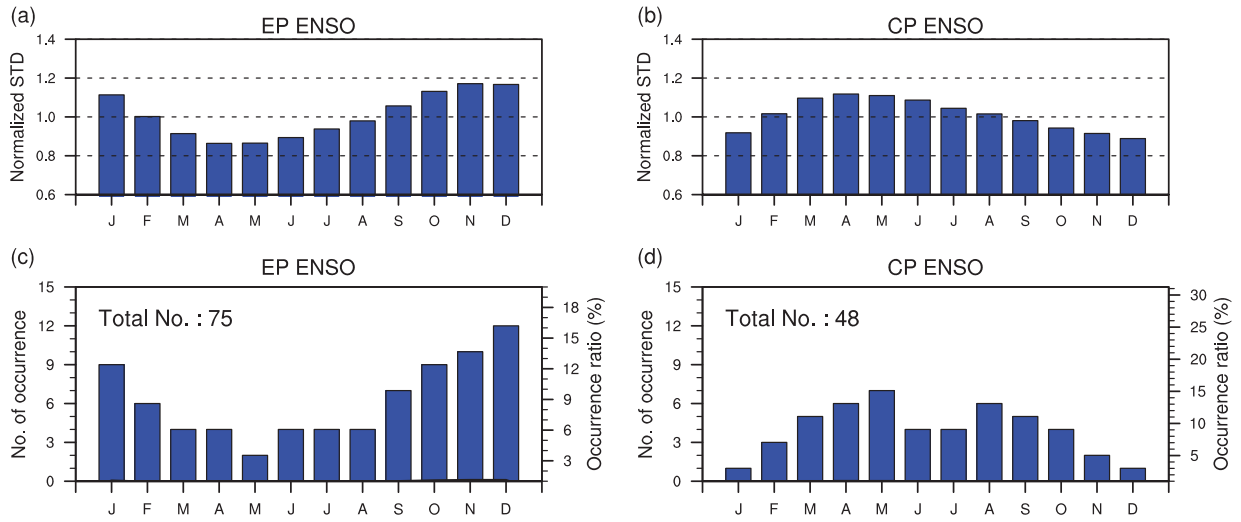

Figure 4. (a, b) The upper panels show the standard deviation of (a) EPC1 and (b) EPC2 indices, obtained from the JA classification method, normalized by the standard deviation for the total month on the variability of each index referenced to calendar months. (c, d) The bottom panels indicate numbers of monthly occurrence (left axis) and the ratio of the number of actual monthly occurrences to the total number of occurrences (right axis) for (c) EP-type and (d) CP-type ENSO events.

phase-locked by the seasonal cycle (Rasmusson and Carpenter, 1982; Kao and Yu, 2009). Kao and Yu (2009) examined phase locking features for EP-type and CP-type ENSO events using composite Niño SST indices, and found that the life cycles of two types of ENSO phase have similar evolution; gradually building up to a peak by the end of a calendar year and rapidly subsiding by next spring.

In this section, based on our classification method, the statistical characteristic related to the phase and frequency locking with respect to calendar months is investigated for two ENSO types. To do this, we used the normalized monthly standard deviation of EPC1 and EPC2 indices divided by the standard deviation of each index for the total month (Neelin *et al.*, 2000; Kao and Yu, 2009; Ham *et al.*, 2013) (Figure 4).

For the EP-type ENSO event of Figure 4(a), the peak of the normalized standard deviation on EPC1 index appears during the cold season, while the minimum occurs during spring such as April and May. The EPC1 index describing the EP-type ENSO shows a tendency for the event, to reach a maximum by the end of the year and become phase-locked to the seasonal cycle (figure not shown). According to Kao and Yu (2009), the life cycles of existing indices of CP-type ENSO events show a very similar evolution to that of EP-type ENSO activities, which indicates a mature phase during winter. However, the normalized variability of the EPC2 index for CP-type ENSO phenomena shows phase-locking behaviour during spring rather than during boreal winter (Figure 4(b)). Figure 4(c) and (d) shows that distributions of the number of occurrences for EP-type and CP-type ENSO events with respect to calendar months are very similar to their phase-locking behaviours in Figure 4(a) and (b), respectively. The total number of occurrences of EP (CP)-type ENSO events is 75 (48) during the whole period from January 1982 to December 2014. The frequency of occurrence of the EP-type ENSO phenomenon in Figure 4(c) is maximized with the value of more than 15% in December and minimized with the value of less than about 3% in May. In contrast, the occurrence rate of CP-type ENSO events in Figure 4(d) is lowest (less than about 2%) in December and January but highest (almost around 15%) in May.

4. Summary and conclusions

In this work, the EPC1 and EPC2 are proposed as new classification indices to divide ENSO events into EP-type and CP-type, respectively. For clear separation of two types of ENSO event, these indices are defined as PCCs between the first two leading EOF modes of SST and observed monthly SSTAs over the tropical Pacific. Based on our new method, we classified ENSO events into EP-type and CP-type El Niño and La Niña events from January 1982 to December 2014 (shown in Table S1, Supporting Information).

Two EPC indices are closely related with two types of ENSO index derived from five existing methods. Our new indices have, however, no overlapping cases between EP-type and CP-type ENSO events, as compared with other indices. The observed composited SSTA field for each ENSO event and the each regressed SST pattern onto two types of ENSO index over the Pacific Ocean are also compared using the spatial pattern correlation. Our results show that distinctive features associated with EP-type and CP-type ENSO events are well described in SST responses to EPC1 and EPC2 indices, respectively. The statistical characteristics are also investigated in terms of the phase locking and the frequency of the occurrence of two types of ENSO event. The variation of our EP-type ENSO (EPC1) index shows a tendency of the highest peak by the end of the year and the phase locking by the seasonal cycle, while the CP-type ENSO (EPC2) index exhibits a significant variation reaching at the mature phase in spring

instead of winter. The monthly frequencies of occurrences derived from two EPC indices for two types of ENSO event are quite similar to variation patterns of phase-locking behaviours. Through the comparison with previous other indices, newly developed indices have been demonstrated their usefulness as a method for clearly classifying ENSO events into EP-type and CP-type.

Further research is required to conduct more detailed analyses related to remote impacts on various atmospheric variables (temperature, precipitation, wind, etc.) over the extratropics and other regions, as well as ENSO prediction, based on two newly defined ENSO indices. Besides this, a new index needs to be developed that indicates the intensity of EP and CP types of ENSO.

Acknowledgements

This work was carried out with the support of the 'Cooperative Research Program for Agriculture Science & Technology Development (Project No. PJ012293)' of Rural Development Administration, Republic of Korea, and the Korea Meteorological Administration Research and Development Program under grant KMIPA 2015-2081.

Supporting Information

The following supporting information is available as part of the online article:

Table S1. EP- and CP-type El Niño and La Niña events from January 1982 to December 2014 defined by EPC1 and EPC2.

References

Ashok K, Behera S, Rao AS, Weng HY, Yamagata T. 2007. El Niño Modoki and its teleconnection. *J. Geophys. Res.* **112**: C11007.

Ashok K, Tam CY, Lee WJ. 2009. ENSO Modoki impact on the Southern Hemisphere storm track activity during extended austral winter. *Geophys. Res. Lett.* **36**: L12705.

Capotondi A, Wittenberg AT, Matthew N, Lorenzo ED, Yu JY, Braconnot P, Cole J, Dewitte B, Giese B, Guilyardi E, Jin FF, Karnauskas K, Kirtman B, Lee T, Schneider N, Xue Y, Yeh WS. 2015. Understanding ENSO diversity. *Bull. Am. Meteorol. Soc.* **96**: 921–938.

Chen G. 2011. How does shifting Pacific Ocean warming modulate on tropical cyclone frequency over the South China Sea? *J. Clim.* **24**: 4695–4700.

Chiodi AM, Harrison DE. 2013. El Nino impacts on seasonal U.S. atmospheric circulation, temperature, and precipitation anomalies: the OLR-event perspective. *J. Clim.* **26**: 822–837.

Feng J, Li J. 2011. Influence of El Niño Modoki on spring rainfall over South China. *J. Geophys. Res.* **116**: D13102.

Ham YG, Kug JS, Kim D, Kim YH, Kim DH. 2013. What controls phase-locking of ENSO to boreal winter in coupled GCMs? *Clim. Dyn.* **40**: 1551–1568.

Jeong HI, Ahn JB, Lee JY, Alessandri A, Hendon HH. 2015. Interdecadal change of interannual variability and predictability of two types of ENSO. *Clim. Dyn.* **44**: 1073–1091.

Jeong HI, Lee DY, Ashok K, Ahn JB, Lee JY, Luo JJ, Schemm JK, Hendon HH, Braganza K, Ham YG. 2012. Assessment of the APCC coupled MME suite in predicting the distinctive climate impacts of two flavors of ENSO during boreal winter. *Clim. Dyn.* **39**: 475–493.

Jolliffe IT, Stephenson DB. 2003. *Forecast Verification: A Practitioner's Guide in Atmospheric Science*. Wiley: New York, NY.

Kao HY, Yu JY. 2009. Contrasting eastern-Pacific and central-Pacific types of ENSO. *J. Clim.* **22**: 615–632.

Kim HM, Webster PJ, Curry JA. 2009. Impact of shifting patterns of Pacific Ocean warming on north Atlantic tropical cyclones. *Science* **325**: 77–80.

Kug JS, Ahn MS, Sung MK, Yeh SW, Min HS, Kim YH. 2010. Statistical relationship between two types of El Niño events and climate variation over the Korean Peninsula. *Asia Pac. J. Atmos. Sci.* **46**: 467–474.

Kug JS, Jin FF, Ahn SI. 2009. Two types of El Niño events: cold tongue El Nino and warm pool El Niño. *J. Clim.* **22**: 1499–1515.

Kumar KK, Rajagopatan B, Hoerling M, Bates G, Cane M. 2006. Unraveling the mystery of Indian monsoon failure during El Niño. *Science* **314**: 115–119.

Larkin NK, Harrison DE. 2005. Global seasonal temperature and precipitation anomalies during El Niño autumn and winter. *Geophys. Res. Lett.* **32**: L16705.

Mo KC. 2010. Interdecadal modulation of the impact of ENSO on precipitation and temperature over the United States. *J. Clim.* **23**: 3639–3656.

Neelin J, Jin FF, Syu HH. 2000. Variations in ENSO phase locking. *J. Clim.* **13**: 2570–2590.

Rasmusson EM, Carpenter TH. 1982. Variations in tropical sea surface temperature and surface wind fields associated with the Southern Oscillation El Niño. *Mon. Weather Rev.* **110**: 354–384.

Ren HL, Jin FF. 2011. Niño indices for two types of ENSO. *Geophys. Res. Lett.* **38**: L04704.

Reynolds RW, Rayner NA, Smith TM, Stokes DC, Wang W. 2002. An improved in situ and satellite SST analysis for climate. *J. Clim.* **15**: 1609–1625.

Singh A, Delcroix T, Cravatte S. 2011. Contrasting the flavors of El Nino and Southern Oscillation using sea surface salinity observations. *J. Geophys. Res.* **116**: C06016, doi: 10.1029/2010JC006862.

Smith TM, Reynolds RW, Peterson TC, Lawrimore J. 2008. Improvements to NOAA's historical merged land-ocean surface temperature analysis (1880–2006). *J. Clim.* **21**: 2283–2296.

Takahashi K, Montecinos A, Goubanova K, Dewitte B. 2011. ENSO regimes: reinterpreting the canonical and Modoki El Niño. *Geophys. Res. Lett.* **38**: L10704.

Taschetto AS, England MH. 2009. El Niño Modoki impacts on Australian rainfall. *J. Clim.* **22**: 3167–3174.

Trenberth KE, Stepaniak DP. 2001. Indices of El Niño evolution. *J. Clim.* **14**: 1697–1701.

Wang G, Hendon HH. 2007. Sensitivity of Australian rainfall to inter-El Niño variations. *J. Clim.* **20**: 4211–4226.

Weng H, Wu G, Liu Y, Behera SK, Yamagata T. 2011. Anomalous summer climate in China influenced by the tropical Indo-Pacific Oceans. *Clim. Dyn.* **36**: 769–782.

Yu JY, Kao HY. 2007. Decadal changes of ENSO persistence barrier in SST and ocean heat content indices: 1958–2001. *J. Geophys. Res.* **112**: D13106.

Yu JY, Kao HY, Lee T, Kim ST. 2011. Subsurface ocean temperature indices for Central-Pacific and Eastern-Pacific types of El Nino and La Nina events. *Theor. Appl. Climatol.* **103**: 337–344.

Zhang W, Jin FF, Li J, Ren HL. 2011. Contrasting impacts of two-type El Niño over the western north Pacific during boreal autumn. *J. Meteorol. Soc. Jpn.* **89**: 563–569.